ELSEVIER

Water-soluble (η6-arene)ruthenium(II)-phosphine complexes and their catalytic activity in the hydrogenation of bicarbonate in aqueous solution

Henrietta Horváth [a], Gábor Laurenczy [b], Ágnes Kathó [a,c,*]

[a] *Institute of Physical Chemistry, University of Debrecen, P.O. Box 7, Debrecen-10 H-4010, Hungary*
[b] *Institut de Chimie Moléculaire et Biologique, Ecole Polytechnique Fédérale de Lausanne, Lausanne CH-1015, Switzerland*
[c] *Research Group of Homogeneous Catalysis, Hungarian Academy of Sciences, P.O. Box 7, Debrecen 10 H-4010, Hungary*

Abstract

The reactions of $[(\eta^6\text{-}C_6H_6)RuCl_2]_2$ and $[(\eta^6\text{-}p\text{-cymene})RuCl_2]_2$ with hydrogen in the presence of the water-soluble phosphines tppts (*meta*-trisulfonated triphenylphosphine) and pta (1,3,5-triaza-7-phosphaadamantane) afforded as the main species $[(\eta^6\text{-}C_6H_6)RuH(tppts)_2]^+$, $[(\eta^6\text{-}C_6H_6)RuH(pta)_2]^+$, $[(\eta^6\text{-}p\text{-cymene})RuH(tppts)_2]^+$ and $[(\eta^6\text{-}p\text{-cymene})RuH(pta)_2]^+$. This latter complex was also formed in the reaction of $[(\eta^6\text{-}p\text{-cymene})RuCl_2(pta)]$ and hydrogen with a redistribution of pta. In addition, prolonged hydrogenation at elevated temperatures and in the presence of excess of pta led to the formation of the arene-free $[RuH(pta)_4Cl]$, $[RuH(pta)_4(H_2O)]^+$, $[RuH_2(pta)_4]$ and $[RuH(pta)_5]^+$ complexes. Ru-hydrides, such as $[(\eta^6\text{-arene})RuH(L)_2]^+$, catalyzed the hydrogenation of bicarbonate to formate in aqueous solutions at $p(H_2) = 100$ bar, $T = 50$–70 °C.
© 2004 Elsevier B.V. All rights reserved.

*Keywords:* (Arene)ruthenium complexes; Carbon dioxide; Hydrogenation; Water-soluble phosphines

1. Introduction

(η6-Arene)ruthenium(II) complexes have been subject to intensive studies for many years due to their interesting coordination chemistry and catalytic properties [1]. Among others, prochiral ketones were reduced with practically complete enantioselectivity with catalysts prepared from $[(\eta^6\text{-arene})RuCl_2]_2$ (arene = mesitylene, *p*-cymene) and asymmetrically substituted diamines [2], and high enantioselectivity was also obtained with amino acids as chiral ligands [3,4]. The $[(\eta^6\text{-arene})RuCl_2(PR_3)]$ complexes obtained in the reaction of $[(\eta^6\text{-arene})RuCl_2]_2$ and tertiary phosphines are widely used for the selective addition of carboxylic acids to alkynes [5]. In the presence of reducing agents, such $[(\eta^6\text{-arene})RuCl_2(PR_3)]$ derivatives easily give $[(\eta^6\text{-arene})RuHCl(PR_3)]$ complexes which act as catalysts of homogeneous hydrogenation of olefins and aromatics [6].

Aqueous-phase organometallic catalysis has attracted much recent interest due to the relatively easy recycling of water-soluble catalysts in aqueous-organic biphasic reaction mixtures [7,8]. Although there are a few known catalytic systems employing water-soluble (η6-arene)ruthenium(II)-derivatives as catalysts, the studies so far were focussed on the catalytic properties of the various cluster species obtained from $[(\eta^6\text{-arene})RuCl_2]_2$ under elevated H_2 pressure [9–11] and on the catalytic properties of $[(p\text{-cymene})RuCl_2]_2$ with water-soluble chiral diamines [12]. However, the chemistry of the $[(\eta^6\text{-arene})RuCl_2(L)]$ complexes with L = water-soluble phosphine ligands (Scheme 1) have remained scarcely explored. In particular, $[(\eta^6\text{-}C_6H_6)RuCl(tppts)_2]Cl$ was prepared from tppts (trisodium 3,3′,3″-phosphinetriylbenzenesulfonate) and $[(\eta^6\text{-}C_6H_6)RuCl_2]_2$ and has been used as catalyst for the hydration of terminal alkynes in 2-methoxyethanol solution [13]. The analogous cationic $[(\eta^6\text{-}p\text{-cymene})RuCl(pta)_2]BF_4$ (pta = 1,3,5-triaza-7-phosphatricyclo [3.3.1.1]decane) as well as the neutral $[(\eta^6\text{-}p\text{-}$
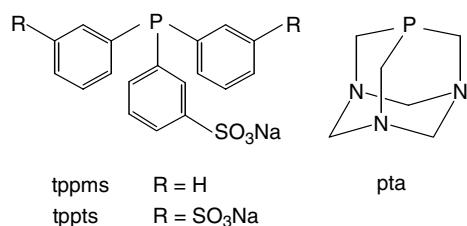
Scheme 1. The water-soluble phosphines used in this study.

cymene)RuCl$_2$(tppts)] and [(η^6-*p*-cymene)RuCl$_2$(pta)] complexes have been used as catalysts for the hydrogenation of benzene and several other arenes [14–16], while [(η^5-C$_5$R$_5$)RuCl(pta)$_2$] (R = H, Me) was found to catalyze the aqueous-organic biphasic hydrogenation of benzylidene acetone [17]. It is of interest to note that in the water–toluene biphasic hydrogenation of aromatic aldehydes using a [{RuCl$_2$(tppts)$_2$}$_2$] catalyst, formation of [(η^6-arene)RuH(tppts)$_2$]$^+$ complexes was unambiguously established at $p(H_2) = 35$ bar and $T = 40$ °C; both the substrate and the toluene solvent could serve as the arene ligand [18].

The catalytic transformation of carbon dioxide into useful products, i.e., the use of this greenhouse gas as a C1 building block is a major challenge in organometallic catalysis. Until now significant results have been achieved in the hydrogenation of CO$_2$ into formic acid derivatives in the presence of amines, using Rh(I)- and Ru(II)-tertiary phosphine catalysts both in organic [19] and in aqueous solutions [20,21], as well as in supercritical CO$_2$ [22,23]. [(η^6-Arene)RuCl$_2$]$_2$ (arene = mesitylene, *p*-cymene) complexes have already been used as catalyst precursors [24,25] in the hydrogenation of CO$_2$ in organic solvents; however, no intermediates of these reactions have been identified.

In order to explore the mechanism of the hydrogenations catalyzed by [(η^6-C$_6$H$_6$)RuCl$_2$(L)] and [(η^6-*p*-cymene)RuCl$_2$(L)] (L = tppts, pta), we have made extensive studies on the reactivity of these complexes towards H$_2$ in aqueous solution, using high gas pressure NMR techniques (up to 100 bar H$_2$). One of the primary aim of this research was to establish the nature and stability of the hydridoruthenium(II) species under the conditions frequently used for catalytic hydrogenations. The catalysis of the hydrogenation of bicarbonate with some of the mentioned water-soluble [(η^6-arene)RuCl$_2$(PR$_3$)] complexes is also reported.

2. Experimental

All manipulations were done in an inert atmosphere, and doubly distilled water was used throughout. RuCl$_3 \cdot 3$H$_2$O was a loan of Johnson Matthey. ^{13}C-enriched (99%) NaHCO$_3$ and D$_2$O (99.9%) were obtained from Cambridge Isotope Laboratories. tppms

(sodium 3-diphenylphosphineylbenzenesulfonate) [26], [{RuCl$_2$ (tppms)$_2$}$_2$] [26], tppts [27], pta [28], [(η^6-C$_6$H$_6$)RuCl$_2$]$_2$ [29], [(η^6-*p*-cymene)RuCl$_2$]$_2$ [30] and [(*p*-cymene) RuCl$_2$(pta)] [14] were prepared according to the literature. [(η^6-C$_6$H$_6$)RuCl$_2$(pta)] was obtained in a synthesis analogous to that of [(*p*-cymene)RuCl$_2$(pta)] [14] as follows. A methanolic solution of [(η^6-C$_6$H$_6$)RuCl$_2$]$_2$ (165 mg, 0.33 mmol) and pta (103 mg, 0.66 mmol) was refluxed for 24 h. Removal of the solvent afforded brown microcrystalline [(η^6-C$_6$H$_6$)RuCl$_2$(pta)] (77 mg, 28%). ^{31}P NMR (0.5 M KCl in D$_2$O): δ (ppm) = −32.12, s. ^{1}H NMR (0.5 M KCl in D$_2$O): δ (ppm) = 5.89 (6H, CH aromatic), 4.58 (6H, N–CH$_2$–N), 4.29 (6H, P–CH$_2$–N). The solid-state structures of [(η^6-C$_6$H$_6$)RuCl$_2$(pta)] (vide infra) and [(*p*-cymene)RuCl$_2$(pta)] were determined by single crystal X-ray diffraction. However, the structure of [(*p*-cymene)RuCl$_2$(pta)] has been published [14] during the preparation of this paper and therefore our data are not included here. All other compounds were high purity products of Sigma–Aldrich and were used as received.

^{1}H and ^{31}P NMR spectra were recorded on a Bruker WP 360 SY or a DRX400 equipment in D$_2$O or D$_2$O/H$_2$O mixtures. Pressurized samples were studied using a thick-wall glass NMR tube with a teflon valve (Aldrich; up to 10 bar) or medium pressure sapphire NMR tubes (up to 100 bar). Chemical shifts are referenced to 2,2-dimethyl-2-silapentane-5-sulfonic acid Na-salt (dss, Fluka) and 85% H$_3$PO$_4$, respectively.

2.1. Hydrogenation of bicarbonate

A medium pressure sapphire NMR tube (o.d. 10 mm) was used as a reactor and a typical experiment was run as follows. In this tube under an N$_2$ atmosphere, 168 mg (2.00 mmol) NaHCO$_3$ (10% ^{13}C), 2.0 mg (0.008 mmol Ru) [(η^6-C$_6$H$_6$)RuCl$_2$]$_2$ and 9.9 mg (0.016 mmol) tppts or 2.6 mg (0.016 mmol) pta were dissolved in 2.0 mL D$_2$O. The reactor was filled with H$_2$ up to the desired pressure. The tube was securely placed on top of a laboratory shaker equipped with a controlled temperature heating block to accomodate the reactor and the reaction mixture was shaken at 60 °C. The reaction was followed by recording the ^{13}C NMR spectra of the solution in time and comparing the integrals of the formate, bicarbonate and carbonate signals. The catalytic activity of [(η^6-*p*-cymene)RuCl$_2$(pta)] was studied the same way using 3.8 mg (0.008 mmol) of the complex.

2.2. Other hydrogenations

The reaction of H$_2$ with [(η^6-*p*-cymene)RuCl$_2$(pta)] or with mixtures of pta or tppms and [(η^6-C$_6$H$_6$)RuCl$_2$]$_2$ or [(η^6-*p*-cymene)RuCl$_2$]$_2$ were studied the same way as described for the hydrogenation of bicarbonate. The

Table 1
Crystal and refinement data for $[(\eta^6\text{-}C_6H_6)RuCl_2(pta)] \cdot H_2O$

Empirical formula	$C_{12}H_{20}Cl_2N_3OPRu$
Formula weight	425.25
Temperature (K)	293
Wavelength (Å)	0.71073
Crystal system	Orthorhombic
Space group	*Pcmn*
Unit cell dimensions	
a (Å)	10.6634(20)
b (Å)	11.2864(20)
c (Å)	13.1333(20)
V (Å^3)	1580.6(2)
Z	4
D_{calc} (Mg m^{-3})	1.787
Absorption coefficient (mm^{-1})	1.429
$F(000)$	856
Crystal size (mm^3)	$0.28 \times 0.25 \times 0.19$
Crystal color	Red
θ range for data collection	2.46–25.38
Index ranges	$0 \leqslant h \leqslant 12$, $0 \leqslant k \leqslant 13$, $0 \leqslant l \leqslant 15$
Reflections collected	1532
Independent reflections	1532 [$R_{int} = 0.00$]
Completeness to $\theta = 25.38°$	99.9%
Absorption correction	Empirical (ψ scan)
Maximum and minimum transmission	0.7618 and 0.7204
Decay (%)	1
Refinement method	Full-matrix least-squares on F^2
Data/restraints/parameters	1532/2/109
Final R indices [all data]	$R_1 = 0.0534$, $wR_2 = 0.1558$
Goodness-of-fit on F^2	1.037
Largest difference peak and hole	0.907 and -1.616 (e Å^{-3})

reactions were followed by taking ^{1}H and ^{31}P NMR spectra with time.

2.3. X-ray crystal structure determination of $[(\eta^6\text{-}C_6H_6)RuCl_2(pta)]$

A brownish red prism of dimensions of 0.28 mm × 0.25 mm × 0.19 mm was mounted on a glass fiber with epoxy cement. Data collection was performed on an Enraf–Nonius MACH3/PC diffractometer in non-profiled $\omega/2\theta$ scans. A total of 1532 independent reflections were collected. The structure was solved with the use of direct methods [31] and refined by using SHELXL 97 [32]. H atoms were treated by a mixture of independent and constrained refinement. Scattering factors for all atoms and anomalous dispersion corrections for the non-hydrogen atoms were taken from [33]. Pertinent crystal and refinement data are shown in Table 1.

3. Results and discussion

3.1. Structure of $[(\eta^6\text{-}C_6H_6)RuCl_2(pta)]$ in the solid state

Determination of the molecular structures of water-soluble phosphine complexes by single crystal X-ray

diffraction is seriously limited by the low crystallinity of these solids. One notable exemption is the case of pta-complexes which can generally yield X-ray quality crystals. Up till now, no $[(\eta^6\text{-}C_6H_6)RuCl_2(L)]$ complexes with L = water-soluble phosphines have been isolated although analogous compounds with *p*-cymene and L = pta and tppts are known [14,15]. The solid-state structures of $[(\eta^6\text{-}C_6H_6)RuCl_2(PPh_3)]$ [34] and $[(\eta^6\text{-}C_6H_6)RuCl_2(PPh_2Me)]$ have also been determined [35]. Here, we briefly report the solid-state structure of $[(\eta^6\text{-}C_6H_6)RuCl_2(pta)]$ (Fig. 1). The compound was obtained in the reaction of $[(\eta^6\text{-}C_6H_6)RuCl_2]_2$ with a stoichiometric amount of pta in methanol, and X-ray quality crystals (containing one H_2O in the lattice) were obtained from a recrystallization in water–methanol.

Expectedly, the solid-state structure of $[(\eta^6\text{-}C_6H_6)RuCl_2(pta)]$ is highly similar to that of $[(\eta^6\text{-}p\text{-}cymene)RuCl_2(pta)]$ [14]. There are two independent molecules in the unit cell, connected by an H_2O. In $[(\eta^6\text{-}C_6H_6)RuCl_2(pta)]$, the average Ru–C and Ru–Cl bonds are 0.05 Å shorter and the Ru–P bond is 0.05 Å longer than the same bonds in $[(\eta^6\text{-}p\text{-}cymene)RuCl_2(pta)]$. There are no greater differences in comparison to $[(\eta^6\text{-}C_6H_6)RuCl_2(PPh_3)]$, either, in which the Ru–Cl bonds are 0.05 Å longer and the Ru–C$_{avr}$ is 0.05 Å shorter than in $[(\eta_6\text{-}C_6H_6)RuCl_2(pta)]$. The largest variation in the bond angles is shown by the P–Ru–C$_{center}$ angle which was determined as 132.7° in $[(\eta_6\text{-}C_6H_6)RuCl_2(pta)]$ in contrast to 129.7° in both $[(\eta^6\text{-}p\text{-}cymene)RuCl_2(pta)]$ and $[(\eta^6\text{-}C_6H_6)RuCl_2(PPh_3)]$. Crystal and refinement data are found in Table 1.

3.2. Reaction of $[(\eta^6\text{-}arene)RuCl_2(PR_3)]$ complexes with H_2 in aqueous solution

$[(\eta^6\text{-}C_6H_6)RuCl_2]_2$ is fairly water-soluble (possibly with formation of $[(\eta^6\text{-}C_6H_6)RuCl_2(H_2O)]$) and already

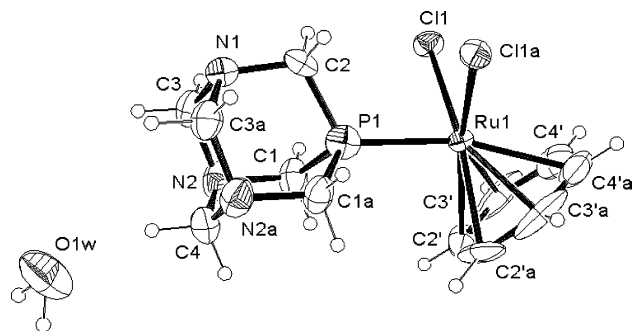Fig. 1. ORTEP view of $[(\eta^6\text{-}C_6H_6)RuCl_2(pta)] \cdot H_2O$ at 40% probability level with numbering scheme. Selected bond length (Å) and angle (°) data. Letter "a" indicates symmetry related atom by x, $1/2 - y$, z. Ru1–P1 2.237(4), Ru1–Cl1 2.4155(18), Ru(1)–C2′ 2.132(8), Ru1–C3′ 2.145(9), Ru1–C4′ 2.191(9); P1–Ru1–Cl1 84.87(9), Cl1–Ru1–Cl1a 89.22(10), C1–P1–Ru1 114.9(3), C2–P1–Ru1 118.6(5), C2′–Ru1–Cl1 116.3 (5), C3′a–Ru1–Cl1 152.4(5) and C4′–Ru1–Cl1 92.5(3).

at low pressures reacts with hydrogen to yield hydrido-cluster compounds [9]. We also used this dimer as a precursor for the in situ formation of the (hydrido)(arene)Ru(II) complexes with the tppts and pta phosphine ligands. In contrast, $[(\eta^6\text{-}p\text{-cymene})RuCl_2]_2$ is much less soluble in water, although it can be dissolved in the presence of water-soluble phosphines with prolonged shaking. Conversely, the readily available $[(\eta^6\text{-}p\text{-cymene})RuCl_2(pta)]$ [14] is more soluble in water than $[(\eta^6\text{-}C_6H_6)RuCl_2(pta)]$, and for that reason it was our choice for detailed studies both in reactions with H_2 and in the catalytic hydrogenation of bicarbonate.

$[(\eta^6\text{-}p\text{-cymene})RuCl_2(pta)]$ dissolves well in chloroform and its ^1H and ^{31}P NMR spectra in this solvent are at variance with that recorded in water. In $CDCl_3$ the ^{31}P NMR spectrum shows the expected singlet ($\delta = -36.6$ ppm), while in D_2O two singlets are observed at $\delta = -35.2$ and -33.9 ppm. On the addition of chloride these two singlets are replaced by a single resonance, $\delta = -36.18$ ppm (s). This novel observation can be explained by the following chloride dissociation equilibrium:

$$[(\eta^6\text{-}p\text{-cymene})RuCl_2(pta)] + H_2O$$
$$\rightleftharpoons [(\eta^6\text{-}p\text{-cymene})RuCl(H_2O)(pta)]^+ + Cl^- \qquad (1)$$
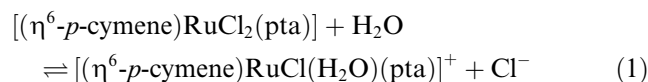
A similar splitting of the ^{31}P NMR signals was observed when the spectra of the complexes obtained in situ from $[(\eta^6\text{-arene})RuCl_2]_2$ and water-soluble phosphines and that of $[(\eta^6\text{-}C_6H_6)RuCl(pta)]$ itself were recorded in D_2O. The ^{31}P NMR data of the $[(\eta^6\text{-arene})RuCl_2(L)]$, $[(\eta^6\text{-arene})RuCl(H_2O)(L)]^+$ and $[(\eta^6\text{-arene})RuCl(L)_2]^+$ are collected in Table 2. With one exception, the data referring to aqueous solutions were determined in this work; for comparison, the relevant literature data for non-aqueous solutions are also shown.
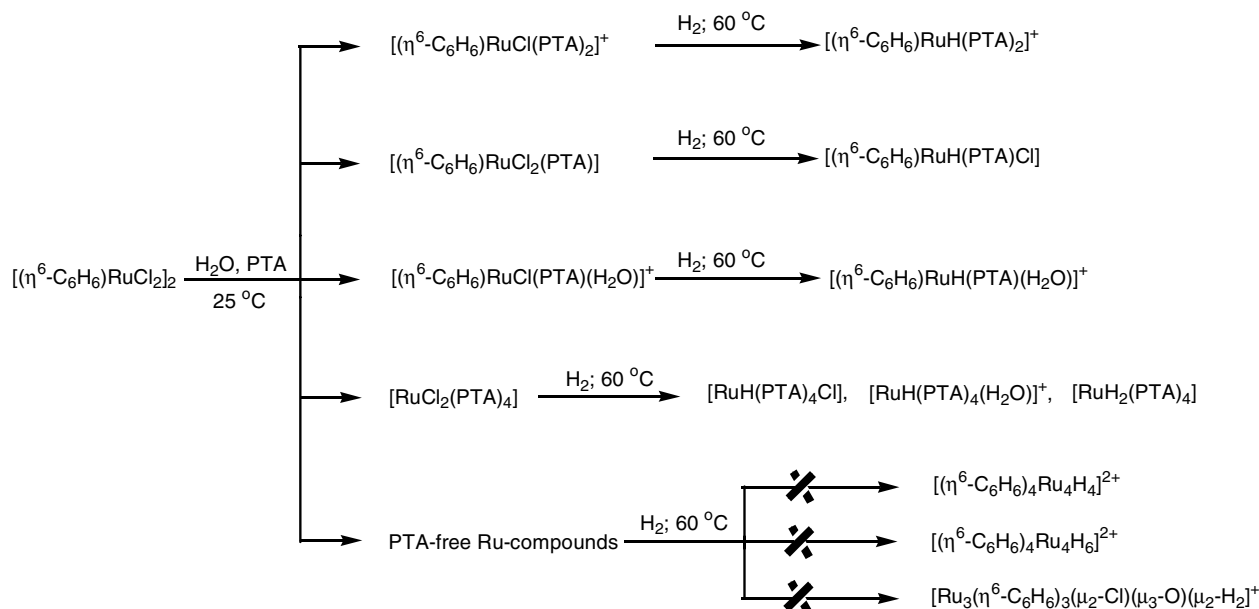
When using tppts as the water-soluble phosphine ligand at a [tppts]/[Ru] ratio of 2, no other complexes than those listed in Table 2 could be detected in the solutions. Conversely, with the pta ligand at the same [pta]/[Ru] ratio, ^{31}P NMR showed the formation of $[RuCl_2(pta)_4]$ the relative amount of which increased with increasing pta excess over Ru (Scheme 2).

The appearance of $[RuCl_2(pta)_4]$ in solutions containing on average 2 pta ligands for 1 Ru requires attention. It is known that in aqueous solutions the arene ligands can be lost, especially at higher temperatures [29] and this opens the way to the formation of tetrakisphosphino complexes. It seems from our measurements that part of the ruthenium becomes invisible for ^{31}P NMR spectroscopy, i.e., it is present in arene-stabilized clusters, such as, e.g., $[Ru_3(\eta^6\text{-}p\text{-cymene})_3(\mu_3\text{-Cl})]^+$ [15] or halo-aqua-complexes.

In the absence of tertiary phosphines, the reaction of $[(\eta^6\text{-}C_6H_6)RuCl_2]_2$ in aqueous solution at 60 °C under 100 bar H_2 yielded the hydrido-clusters, $[Ru_4H_4(\eta^6\text{-}C_6H_6)_4]^{2+}$ and $[Ru_4H_6(\eta^6\text{-}C_6H_6)_4]^{2+}$, described earlier by Süss-Fink [9]; there was no sign of other clusters such as $[Ru_3(\eta^6\text{-}C_6H_6)_3(\mu_2\text{-Cl})(\mu_3\text{-O})(\mu_2\text{-H}_2)]^+$ [38]. In the presence of the appropriate water-soluble phosphines, the characteristic ^1H NMR signals of these complexes are replaced by triplets (singlets in the $^1H\{^{31}P\}$ NMR) indicating the formation of $[(\eta^6\text{-}C_6H_6)RuH(tppts)_2]^+$ and $[(\eta^6\text{-}C_6H_6)RuH(pta)_2]^+$. Similarly, under the same conditions, $[(\eta^6\text{-}p\text{-cymene})RuH(tppts)_2]^+$ was formed from $[(\eta^6\text{-}p\text{-cymene})RuCl_2]_2$ and tppts, as well as $[(\eta^6\text{-}p\text{-cymene})RuH(pta)_2]^+$ from $[(\eta^6\text{-}p\text{-cymene})RuCl_2(pta)]$ and pta. The ^1H and ^{31}P NMR data of $[(\eta^6\text{-arene})RuH(L)_2]^+$ complexes are shown in Table 3. Hernandez and Kalck [18] have prepared $[(\eta^6\text{-}C_6H_6)RuH(tppts)_2]^+$ in the reaction of $[\{RuCl_2(tppts)_2\}_2]$ and benzene under hydrogen; the ^1H NMR data for the compounds prepared by the two routes are in perfect match (Table 3). With an other water-soluble phosphine, tppms, we also have detected the formation of $[(\eta^6\text{-}C_6D_6)RuH(tppms)_2]^+$ and $[(\eta^6\text{-toluene})RuH(tppms)_2]^+$ from $[\{RuCl_2(tppms)_2\}_2]$ and the appropriate arene under H_2; the relevant data are included in Table 3.

In accordance with the literature [18], the $^{31}P\{^1H\}$ NMR spectra consisted of a singlet resonance around 55 ppm (complexes with tppms or tppts) and around -15 ppm (complexes with pta), respectively. The NMR spectral features agree with the general structure of these complexes as shown in Scheme 3.

Depending on the [L]/[Ru] ratio, the temperature, the hydrogen pressure and on the time of the exposure to H_2, various further species could be detected in the solutions. Although $[(\eta^6\text{-}C_6H_6)RuH(tppts)_2]^+$ was found stable at 40 °C under 35 bar H_2 [18], when $[(\eta^6\text{-}p\text{-cymene})RuCl_2(tppts)]$ (with no further tppts added) was applied for the hydrogenation of various arenes (90 °C,

Table 2
^{31}P NMR data of $[(\eta^6\text{-arene})RuCl_2(L)]$ and $[(\eta^6\text{-arene})RuCl(L)_2]^+$ in D_2O and other solvents

	D_2O (KCl solution)	Non-aqueous solvent
$[(\eta^6\text{-}C_{10}H_{14})RuCl_2(pta)]$	−33.89; −35.21 (−36.18)	−36.24 (CDCl₃) [16]
$[(\eta^6\text{-}C_{10}H_{14})RuCl(pta)_2]^+$	−32.47	−32.97 (CDCl₃) [15]
$[(\eta^6\text{-}C_6H_6)RuCl_2(pta)]$	−27.61; −29.16 (−32.12)	−31.29 {(D₃C)₂SO} [36]
$[(\eta^6\text{-}C_6H_6)RuCl(pta)_2]^+$	−30.48	
$[(\eta^6\text{-}C_{10}H_{14})RuCl_2(tppms)][37]$		33.84 (CDCl₃)
$[(\eta^6\text{-}C_{10}H_{14})RuCl_2(tppts)]$	34.36; 30.23 34.81; 29.92 [15]	
$[(\eta^6\text{-}C_{10}H_{14})RuCl(tppts)_2]^+$	24.52	
$[(\eta^6\text{-}C_6H_6)RuCl_2(tppts)]$	34.38; 32.35	
$[(\eta^6\text{-}C_6H_6)RuCl(tppts)_2]^+$	24.71	25.3 (CDCl₃) [13]

Scheme 2. Products of the reaction of $[(\eta^6\text{-}C_6H_6)RuCl_2]_2$ and pta in aqueous solution and their further reactions under H_2 pressure ($p = 100$ bar).

Table 3
$^1H\{^{31}P\}$ and $^{31}P\{^1H\}$ NMR data of $[(\eta^6\text{-arene})RuH(L)_2]^+$ complexes[a]

Arene	L	$^1H\{^{31}P\};\delta$ (ppm)	$^{31}P\{^1H\};\delta$ (ppm)	$^2J_{P-H}$ (Hz)	Ref.
Benzene	PPh$_3$	−9.0	n.d	36	[39,40]
Benzene	tppts	−9.34	55.2	36	[b]
		−9.43	55.1	36	[18]
p-cymene	tppts	−9.60	55.3	37	[b]
Benzene-d$_6$[c]	tppms	−9.43	55.5	37	[b]
Toluene [c]	tppms	−9.20	55.2	37	[b]
Benzene	pta	−11.92	−15.0	40	[b]
p-cymene	pta	−12.37	−15.1	40	[b]

  n.d., no data.
[a] All measurements were made in D$_2$O at $T = 40$ °C. All signals are singlets.
[b] This work.
[c] Prepared from $[\{RuCl_2(tppms)_2\}_2]$, H_2 and the appropriate arene following the method described in [18].

60 bar H_2), the catalytic activity was mostly attributed to a colloidal catalyst [15]. We therefore focussed our attention on the behavior of $[(\eta^6\text{-}C_6H_6)RuCl_2(pta)]$ and $[(\eta^6\text{-}p\text{-cymene})RuCl_2(pta)]$.

As mentioned earlier, hydrogenation of $[(\eta^6\text{-}C_6H_6)RuCl_2]_2$ in aqueous solution (60 °C, 100 bar H_2) yielded the known [9] hydrido-clusters $[Ru_4H_4(\eta^6\text{-}C_6H_6)_4]^{2+}$ and $[Ru_4H_6(\eta^6\text{-}C_6H_6)_4]^{2+}$. However, addi-
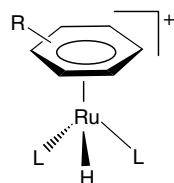
Scheme 3. General structure of the $[(\eta^6\text{-arene})RuH(L)_2]^+$ complexes.

tion of pta, already in a sub-stoichiometric quantity, completely prevented the formation of these hydrido-clusters. Although in solutions with [pta]/[Ru] = 1 $[(\eta^6\text{-}C_6H_6)RuH(pta)_2]^+$ was the dominant hydride species, two additional doublets were observed by ^1H NMR spectroscopy at $\delta = -10.24$ and -10.34 ppm (singlets in $^1H\{^{31}P\}$ NMR, in both cases $^2J_{P-H} = 40$ Hz) which can be assigned to $[(\eta^6\text{-arene})RuH(pta)X]^{n+}$, X = Cl$^-$ ($n = 0$) or H_2O ($n = 1$). At [pta]/[Ru] = 2, $[(\eta^6\text{-}C_6H_6)RuH(pta)_2]^+$ still remained the main hydride species, nevertheless, in longer reaction time the characteristic signals of $[RuH(pta)_4X]^{n+}$ (X = Cl$^-$, $n = 0$; X = H_2O, $n = 1$), described in [21], could also be observed.

We studied the formation of hydrides at the [pta]/[Ru] = 2 ratio at various temperatures and hydrogen pressures. It is important to note that at 60 °C the lower pressure limit for the formation of Ru-hydrides from $[(\eta^6\text{-}C_6H_6)RuCl_2]_2$ and pta was found to be 12 bar. On

the other hand, in solutions under 100 bar H_2, at 40 °C the only hydride species present was $[(\eta_6\text{-}C_6H_6)RuH(pta)_2]^+$. The reaction had to be run at least at 60 °C in order to observe the formation of $[RuH(pta)_4X]^{n+}$. Further increase of the reaction temperature to 80 °C lead to the dominance of the arene-free complexes $[RuH(pta)_4X]^{n+}$ and $[RuH_2(pta)_4]$ [21]. The possible reactions are shown in Scheme 2. It is important to note that the formation of the arene-free ruthenium hydrides requires a rather long induction period. Recorded at 60 °C and under 100 bar H_2 pressure, the ^1H NMR spectra (Fig. 2) clearly show that in the first 90 min, the sole species present in detectable concentration is $[(\eta^6\text{-}C_6H_6)RuH(pta)_2]^+$ (**A**). $[(\eta^6\text{-}C_6H_6)RuH(pta)X]^{n+}$ (**B**) and $[RuH(pta)_4X]^{n+}$ (**C**) appear later and simultaneously as a result of the loss of the arene and redistribution of the pta ligands. At the same temperature and pressure conditions but with [pta]/[Ru] = 3 or 4, after longer reaction times we could also observe the formation of $[RuH_2(pta)_4]$.

Similar observations were made in the reaction of $[(\eta^6\text{-}p\text{-cymene})RuCl_2(pta)]$ and H_2 at 60 °C, 100 bar H_2. In addition to $[(\eta^6\text{-}p\text{-cymene})RuH(pta)_2]^+$, two doublets in the ^1H NMR spectra ($\delta = -10.35$ and -10.43 ppm, singlets in $^1H\{^{31}P\}$ NMR, in both cases $^2J_{P-H} = 40$ Hz) showed the presence of $[(\eta^6\text{-}p\text{-cymene})RuH(pta)X]^{n+}$. Initially the solutions displayed an orange color which in a few hours turned dark. In contrast, addition of pta ($[pta]_{total}/[Ru] = 2$) prevented this color change. In these latter solutions, the only species observed by ^1H NMR spectroscopy was $[(\eta^6\text{-}p\text{-cymene})RuH(pta)_2]^+$ and that could be detected already at 5 bar H_2 pressure at 60 °C.

At $[pta]_{total}/[Ru] = 3$, $[(\eta^6\text{-}p\text{-cymene})RuH(pta)_2]^+$ (**A**) was dominant only in the first 2 h of the reaction; in longer reaction times the known $[RuH(pta)_4X]^{n+}$ (**C**) and $[RuH_2(pta)_4]$ (**D**) complexes could be identified together with minor amounts of $[RuH(pta)_5]^+$ [21]. These reactions were slow and after 20 h $[(\eta^6\text{-}p\text{-cymene})RuH(pta)_2]^+$ still represented approximately 50% of all Ru-hydrides in the solution (Fig. 3).

Upon a further increase of the phosphine concentration, at $[pta]_{total}/[Ru] = 4$, the arene-free $[RuH(pta)_4X]^{n+}$ appeared already in the early stage of the reaction and amounted to about 25% of the dominant $[(\eta^6\text{-}p\text{-cymene})RuH(pta)_2]^+$ species. This latter complex was gradually replaced by $[RuH_2(pta)_4]$ and $[RuH(pta)_5]^+$. After 7 h, the approximate distribution of the Ru-hydrides was $[RuH_2(pta)_4]$ and $[RuH(pta)_5]^+$ 40–40%, $[RuH(pta)_4X]^{n+}$ and $[(\eta^6\text{-}p\text{-cymene})RuH(pta)_2]^+$ 10–10%. During the reaction, the orange solutions turned light yellow, in accordance with the known color [21] of $[RuH_2(pta)_4]$ and $[RuH(pta)_5]^+$.

3.3. Hydrogenation of carbon dioxide and bicarbonate in aqueous solution

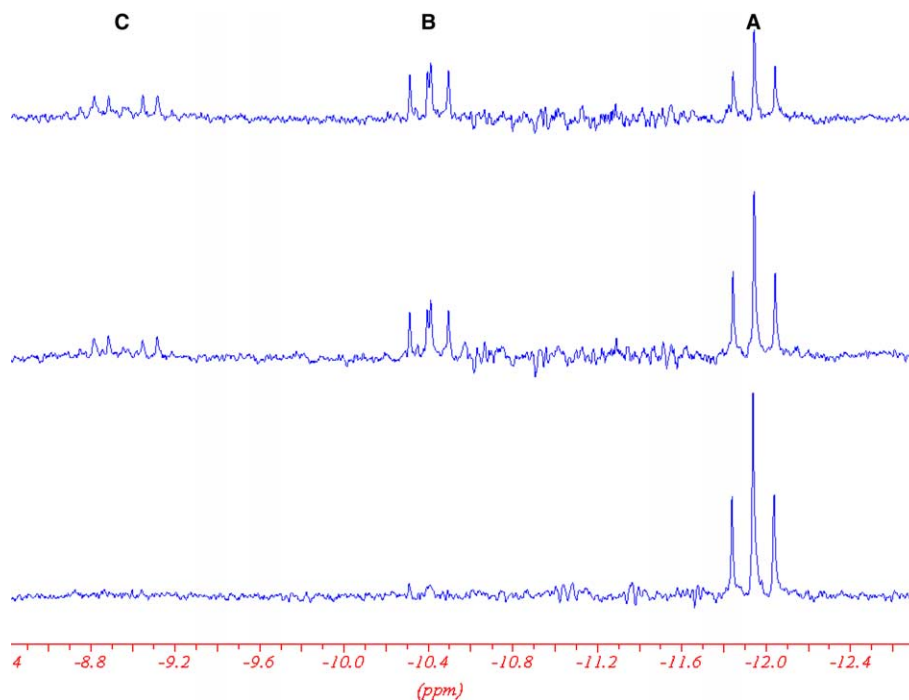The hydrogenation of carbon dioxide is of great interest because of its possible use as a C1 source and also

Fig. 2. ^1H NMR spectra of aqueous solutions of $[(\eta^6\text{-}C_6H_6)RuCl_2]_2$ and pta under hydrogen at various reaction times. [Ru] = 1.4 mM, [pta] = 2.8 mM, $T = 60$ °C, $p(H_2) = 100$ bar, $t = 90$ min (bottom), $t = 180$ min (middle), $t = 270$ min (top), $\mathbf{A} = [(\eta^6\text{-}C_6H_6)RuH(pta)_2]^+$, $\mathbf{B} = [(\eta^6\text{-}C_6H_6)RuH(pta)X]^{n+}$ and $\mathbf{C} = [RuH(pta)_4X]^{n+}$ ($X = Cl^-$, $n = 0$; $X = H_2O$, $n = 1$).
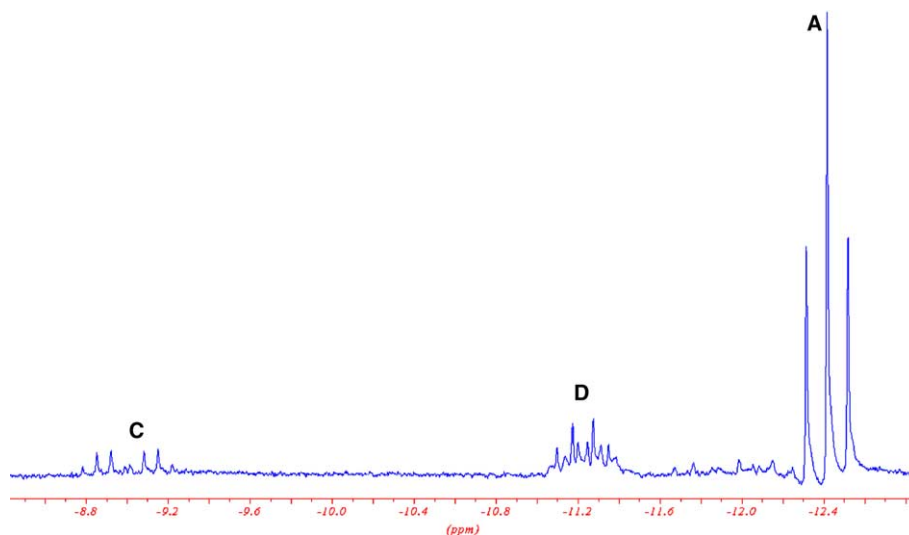
Fig. 3. ^1H NMR spectra of aqueous solutions of [(η^6-p-cymene)RuCl$_2$(pta)] and pta under hydrogen at $t = 20$ h. [Ru] = 7 mM, [pta] = 21 mM, $T = 60$ °C, $p(H_2) = 100$ bar, **A** = [(η^6-C$_6$H$_6$)RuH(pta)$_2$]$^+$, **C** = [RuH(pta)$_4$X]$^{n+}$ (X = Cl$^-$, $n = 0$; X = H$_2$O, $n = 1$) and **D** = [RH$_2$(pta)$_4$].

due to environmental concerns [41]. Several very active homogeneous catalysts are known, including [RuCl$_2$(PMe$_3$)$_4$] [22], working in organic solvents or in supercritical carbon dioxide. It has also been reported that CO$_2$ and HCO$_3^-$ were reduced to formic acid and formate in fully aqueous solutions using [{RuCl$_2$(tppms)$_2$}$_2$] [42] and [RuCl$_2$(pta)$_4$] [21] as catalysts. We wanted to learn the effect of the η^6-arene substitution on the catalytic properties of such Ru(II)-phosphine complexes and therefore studied the hydrogenation of bicarbonate (Eq. (2)) by the species formed under hydrogen from [(η^6-p-cymene)RuCl$_2$(pta)] as well as from [(η^6-C$_6$H$_6$)RuCl$_2$]$_2$ and pta mixtures

$$HCO_3^- + H_2 \rightarrow HCO_2^- + H_2O \qquad (2)$$
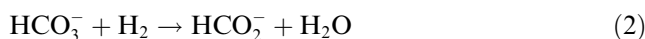
The reactions were followed by ^{13}C NMR spectroscopy using D$_2$O as solvent; formate was detected as the only product of the hydrogenation. In the first few minutes only the signal of HCOO$^-$ was observed ($\delta = 170.8$ ppm, $^1J_{C-H} = 195.9$ Hz) followed by the appearance of the ^{13}C resonance of DCOO$^-$ ($\delta = 170.7$ ppm, $^1J_{C-D} = 30.5$ Hz). During the reaction the concentrations of HCOO$^-$ and DCOO$^-$ became approximately equal; at 80 °C this required less than an hour. Such a fast catalytic deuterium exchange on the formate carbon is not surprising in the light of the high catalytic activity of Ru-phosphine complexes in the H–D exchange reaction in water [43]. The combined integrals of the HCOO$^-$ and DCOO$^-$ resonances related to the signal of HCO$_3^-$ were used to characterize the progress of the reaction. A characteristic kinetic curve is shown in Fig. 4.

The initial reaction rates were determined from the slope of the curves at time zero and are expressed as catalyst turnover frequencies, TOF = mol product (mol
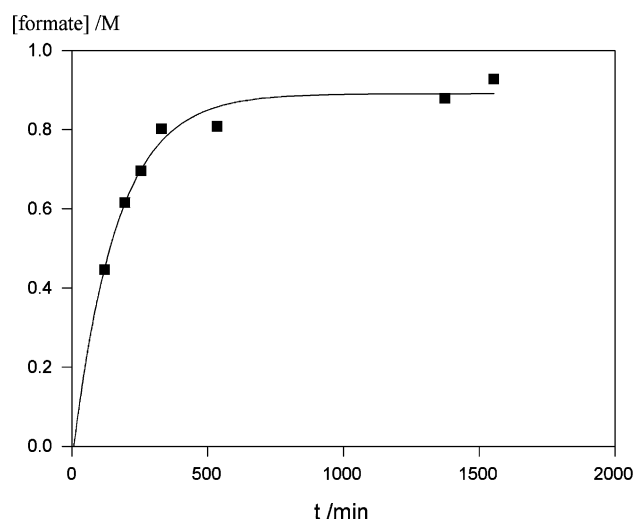

Fig. 4. Hydrogenation of bicarbonate to formate in aqueous solution catalyzed by an in situ formed (arene)ruthenium hydride catalyst. [[(η^6-C$_6$H$_6$)RuCl$_2$]$_2$] = 1 mM, [pta] = 4 mM, [HCO$_3^-$] = 1 M, $T = 60$ °C and $p(H_2) = 100$ bar.

Ru h)$^{-1}$. It is important to note that in no case was an induction period observed. This is in sharp contrast to the bicarbonate hydrogenations catalyzed by [RuCl$_2$(pta)$_4$], where it was necessary to run the reactions at 80 °C in order to avoid induction periods [21].

Under typical experimental conditions (see legend to Table 4), the catalytic activity of the [(η^6-C$_6$H$_6$)RuCl$_2$]$_2$ + pta in situ formed catalyst varied only slightly with the [pta]/[Ru] ratio: at 1/1 the turnover frequency was 67 h^{-1}, while at [pta]/[Ru] = 2/1, it attained TOF = 91 h^{-1}. In comparison, the catalytic activity of the [(η^6-C$_6$H$_6$)RuCl$_2$]$_2$ + tppts system at [tppts]/[Ru] = 2/1 was found to be 25 h^{-1}. The variation of the

Table 4
The catalytic activity of the $[(\eta^6\text{-}C_6H_6)RuCl_2]_2 + 4$ pta in situ formed catalyst in the hydrogenation of HCO_3^- as a function of temperature

T (°C)	TOF (h^{-1})
50	22
60	91
70	237
80	409

Conditions: [Ru] = 2 mM, [pta] = 4 mM, $[HCO_3^-]$ = 1 M and $p(H_2)$ = 100 bar.

turnover frequency with the temperature is shown in Table 4.

From the data in Table 4, an apparent activation energy, $E_a = 126$ kJ mol^{-1} can be calculated. Obviously, this value reflects the temperature sensitivity of a complex reaction and presently no data are available which would allow the identification of one or more of the elementary steps (formation of the catalyst, hydrogen activation, hydride transfer to bicarbonate, etc.) making major contributions to the activation energy. For comparison, the apparent activation energy of the hydrogenation of bicarbonate with a $[RuCl_2(pta)_4]$ catalyst was found to be 86 kJ mol^{-1} [21], while for the $[RhCl(tppts)_3]$-catalyzed hydrogenation of CO_2 in $H_2O/HNMe_2$ mixtures, a much lower value, $E_a = 25$ kJ mol^{-1}, was determined [44].

Jessop and co-workers [25] have screened the activity of the catalysts formed in situ from $[(\eta^6\text{-}C_6H_6)RuCl_2]_2$ and a total of 44 different phosphines in the hydrogenation of CO_2 in 1/1 v/v mixtures of methanol and tripropylamine; the reactions were run at 50 °C under 40 bar H_2 with a total pressure of 100 bar. It is worth mentioning that tppts belonged to the group of phosphines which provided low catalytic activity; with a [tppts]/[Ru] = 3 combination a TOF = 52 h^{-1} was obtained. Although not directly comparable, this value is close to the TOF observed in this study for the hydrogenation of aqueous bicarbonate (25 h^{-1}).

We have also studied the activity of $[(\eta^6\text{-}p\text{-cymene})RuCl_2(pta)]$ in the hydrogenation of HCO_3^-. This complex does not necessarily require the presence of additional pta, nevertheless the catalytic activity increases with increasing pta concentration (Table 5). Interestingly, $[(\eta^6\text{-}p\text{-cymene})RuCl_2(pta)]$ itself did not

Table 5
The catalytic activity of $[(\eta^6\text{-}p\text{-cymene})RuCl_2(pta)]$ in the hydrogenation of aqueous NaHCO$_3$ as a function of the [pta]$_{total}$/[Ru] ratio

[pta]$_{total}$/[Ru]	TOF (h^{-1})
1	139
2	207
3	287

Conditions: [Ru] = 2 mM, $[HCO_3^-]$ = 1 M, $p(H_2)$ = 100 bar and T = 70 °C.

catalyze the formation of deuterated formate; under the conditions given in Table 5, no DCOO$^-$ was detected by ^{13}C NMR spectroscopy after 200 min. Conversely, in the presence of 1 equivalent pta, the [DCOO$^-$]/[HCOO$^-$] ratio reached 0.6 in the same reaction time. With yet another equivalent of pta this [DCOO$^-$]/[HCOO$^-$] did not change, however, the time required for equilibration dropped to 45 min.

Comparison of the relevant data in Tables 4 and 5 shows that the catalysts formed from $[(\eta^6\text{-}C_6H_6)RuCl_2]_2$ are approximately as active as the ones obtained from $[(\eta^6\text{-}p\text{-cymene})RuCl_2(pta)]$. Furthermore, this activity is comparable to that of $[RuCl_2(pta)_4]$ characterized by TOF = 35 h^{-1} ($[HCO_3^-]$ = 1 M, $p(H_2)$ = 100 bar, T = 50 °C) [21].

4. Conclusions and comments on the possible catalytic species

In this work we have shown that the complexes formed in the presence of excess pta from both $[(\eta^6\text{-}C_6H_6)RuCl_2]_2$ and $[(\eta^6\text{-}p\text{-cymene})RuCl_2(pta)]$ catalyze the hydrogenation of NaHCO$_3$ in aqueous solutions. ^{1}H and ^{31}P NMR spectroscopy measurements have revealed that the same starting materials yield cationic hydrido-complexes of the formula $[(\eta^6\text{-arene})RuH(pta)_2]^+$. The monophosphine complexes $[(\eta^6\text{-}C_6H_6)RuHCl(pta)]$ and $[(\eta^6\text{-}C_6H_6)RuH(H_2O)(pta)]^+$ were also detected at low pta concentrations. In addition, further reactions of these complexes at T = 60 °C and $p(H_2)$ = 100 bar lead to the slow formation of $[RuH(pta)_4Cl]$, $[RuH(pta)_4(H_2O)]^+$, $[RuH_2(pta)_4]$ and $[RuH(pta)_5]^+$, especially in the cases with [pta]/[Ru] > 2. It has been shown earlier [21] that the most probable catalytic intermediate in the $[RuCl_2(pta)_4]$-catalyzed hydrogenation of aqueous bicarbonate was $[RuH(pta)_4X]^{n+}$, consequently, its possible role should be considered in our reactions, too. Nevertheless, there are good reasons to regard this role as minor compared to the catalytic activity to the $(\eta^6\text{-arene})$ruthenium hydrides. At the phosphine/ruthenium ratios (mostly 2) used in the catalytic experiments, formation of the $[(\eta^6\text{-arene})RuH(pta)_2]^+$ complexes is instantaneous while that of the arene-free complexes is slow; still the hydrogenations of HCO_3^- proceed with no induction periods. We have also demonstrated that both $[(\eta^6\text{-}C_6H_6)RuH(pta)_2]^+$ and $[(\eta^6\text{-}p\text{-cymene})RuH(pta)_2]^+$ prevailed for several hours as the major hydride species, during which the hydrogenation of bicarbonate attained approximately 70% conversion (Figs. 2 and 3). We do not have enough evidence to discuss in detail the possible catalytic cycle, but think that an ion-pairing interaction of the cationic catalyst and the anionic substrate can be an important step preceding the intermolecular hydride transfer from the ruthenium to the
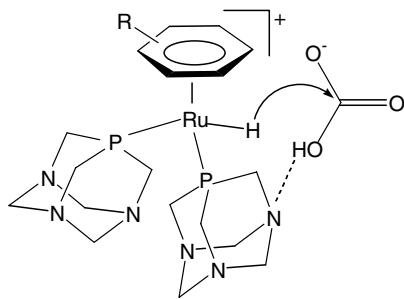
Fig. 5. Possible catalyst substrate interactions during the hydrogenation of HCO_3^- in aqueous solution.

carbon of HCO_3^-. This can be further assisted by formation of a hydrogen bond between one of the nitrogen atoms in the pta ligand and bicarbonate. The suggested intermediate structure is depicted in Fig. 5. Further studies to clarify the mechanistic details of these hydrogenations are in progress in our laboratories.

5. Supplementary material

Crystallographic data for the structural analysis has been deposited with the Cambridge Crystallographic Data Centre, CCDC No. 209767 for compound [(η^6-C_6H_6)RuCl$_2$(pta)]. Copies of this information may be obtained free of charge from The Director, CCDC, 12 Union Road, Cambridge CB2 1EZ, UK (fax: +44-1223-336033; deposit@ccdc.cam.ac.uk or www.ccdc.cam.ac.uk.

Acknowledgements

References

[1] M.A. Bennett, Coord. Chem. Rev. 166 (1997) 225.
[2] R. Noyori, S. Hashiguchi, Acc. Chem. Res. 30 (1997) 97.
[3] D. Carmona, F.J. Lahoz, R. Atencio, L.A. Oro, M.P. Lamata, F. Viguri, E. San José, C. Vega, J. Reyes, F. Joó, Á. Kathó, Chem. Eur. J. 5 (1999) 1544.
[4] Á. Kathó, D. Carmona, F. Viguri, C.D. Remacha, J. Kovács, F. Joó, L.A. Oro, J. Organomet. Chem. 593-594 (2000) 299.
[5] C. Bruneau, P.H. Dixneuf, Chem. Commun. (1997) 507.
[6] M.A. Bennett, T.-N. Huang, A.K. Smith, T.W. Turney, J. Chem. Soc., Chem. Commun. (1978) 582.
[7] F. Joó, Aqueous Organometallic Catalysis, Kluwer, Dordrecht, The Netherlands, 2001.
[8] B. Cornils, W.A. Herrmann (Eds.), Aqueous-Phase Organometallic Catalysis, Wiley-VCH, Weinheim, Germany, 1998.
[9] G. Süss-Fink, A. Meister, G. Meister, Coord. Chem. Rev. 143 (1995) 97.
[10] F. Chérioux, A. Maisse-Francois, A. Neels, H. Stoeckli-Evans, G. Süss-Fink, J. Chem. Soc., Dalton Trans. (2001) 2184.
[11] G. Süss-Fink, M. Faure, T.R. Ward, Angew. Chem., Int. Ed. 41 (2002) 99.
[12] C. Bubert, J. Blacker, S.M. Brown, J. Crosby, S. Fitzjohn, J.P. Muxworthy, T. Thorpe, J.M.J. Williams, Tetrahedon Lett. 42 (2001) 4037.
[13] M. Tokunaga, T. Suzuki, N. Koga, T. Fukushima, A. Horiuchi, Y. Wakatsuki, J. Am. Chem. Soc. 123 (2001) 11917.
[14] C.S. Allardyce, P.J. Dyson, D.J. Ellis, S.L. Heath, Chem. Commun. (2001) 1396.
[15] P.J. Dyson, D.J. Ellis, G. Laurenczy, Adv. Synth. Catal. 345 (2003) 211.
[16] C.S. Allardyce, P.J. Dyson, D.J. Ellis, P.A. Salter, R. Scopelliti, J. Organomet. Chem. 668 (2003) 35.
[17] D.N. Akbayeva, L. Gonsalvi, W. Oberhauser, M. Peruzzini, F. Vizza, P. Brüggeller, A. Romerosa, A. Bergamo, Chem. Commun. (2003) 264.
[18] M. Hernandez, P. Kalck, J. Mol. Catal. A 116 (1997) 131.
[19] P.G. Jessop, T. Ikariya, R. Noyori, Chem. Rev. 95 (1995) 259.
[20] F. Gassner, W. Leitner, J. Chem. Soc., Chem. Commun. (1993) 1465.
[21] G. Laurenczy, F. Joó, L. Nádasdi, Inorg. Chem. 39 (2000) 5083.
[22] P.G. Jessop, Y. Hsiao, T. Ikariya, R. Noyori, J. Am. Chem. Soc. 118 (1996) 344.
[23] Y. Kayaki, Y. Shimokawatoko, T. Ikariya, Adv. Synth. Catal. 345 (2003) 175.
[24] D.J. Drury, J.E. Hamlin, USP 4,474,959, to BP Chemical Ltd.
[25] C-C. Tai, J. Pitts, J.C. Linehan, A.D. Main, P. Munshi, P.G. Jessop, Inorg. Chem. 41 (2002) 1606.
[26] F. Joó, J. Kovács, Á Kathó, A.C. Bényei, T. Decuir, D.J. Darensbourg, Inorg. Synth. 32 (1998) 1.
[27] W.A. Herrmann, C.W. Kohlpaintner, Inorg. Synth. 32 (1998) 8.
[28] D.J. Daigle, Inorg. Synth. 32 (1998) 40.
[29] R.A. Zelonka, M.C. Baird, Can. J. Chem. 50 (1972) 3063.
[30] M.A. Bennett, A.K. Smith, J. Chem. Soc., Dalton Trans. (1974) 233.
[31] A. Altomare, G. Cascarano, C. Giacovazzo, A. Guagliardi, J. Appl. Crystallogr. 26 (1993) 343.
[32] G.M. Sheldrick, SHELXL 97, Program for Crystal Structure Refinement, University of Göttingen, 1997.
[33] A.J.C. Wilson (Ed.), International Tables for Crystallography, vol. C, Kluwer, Dordrecht, The Netherlands, 1992.
[34] M.R.J. Elsegood, D.A. Tocher, Polyhedron 14 (1995) 3147.
[35] M.A. Bennett, G.B. Robertson, A.K. Smith, J. Organomet. Chem. 43 (1972) C41.
[36] P.J. Dyson, personal communication.
[37] The synthesis and properties of [(η^6-$C_{10}H_{14}$)RuCl$_2$(tppms)] will be reported elsewhere.
[38] E.G. Fidalgo, L. Plasseraud, G. Süss-Fink, J. Mol. Catal. A 132 (1998) 5.
[39] D.J. Cole-Hamilton, R.J. Young, G. Wilkinson, J. Chem. Soc., Dalton Trans. (1976) 1995.
[40] O.S. Sisodia, A.N. Sahay, D.S. Pandey, U.C. Agarwala, N.K. Jha, P. Sharma, A. Toscano, A. Cabrera, J. Organometal. Chem. 560 (1998) 35.
[41] H. Arakawa, M. Aresta, J.N. Armor, M.A. Barteu, E.J. Beckman, A.T. Bell, J.E. Bercaw, C. Creutz, E. Dinjus, D.A. Dixon, K. Domen, D.L. DuBois, J. Eckert, E. Fujita, D.H. Gibson, W.A. Goddard, D.W. Goodman, J. Keller, G.J. Kubas, H.H. Kung, J.E. Lyons, L.E. Manzer, T.J. Marks, K. Morokuma, K.M.

Nicholas, R. Periana, L. Que, J. Rostrup-Nielson, W.M.H. Sachtler, L.D. Schmidt, A. Sen, G.A. Somorjai, P.C. Stair, B.R. Stults, W. Tumas, Chem. Rev. 101 (2001) 953.

[42] F. Joó, G. Laurenczy, L. Nádasdi, J. Elek, Chem. Commun. (1999) 971.

[43] G. Kovács, L. Nádasdi, G. Laurenczy, F. Joó, Green Chem. 5 (2003) 213.

[44] W. Leitner, E. Dinjus, F. Gassner, in: B. Cornils, W.A. Herrmann (Eds.), Aqueous-Phase Organometallic Catalysis, Wiley-VCH, Wienheim, Germany, 1998, p. 486.